Syntheses, Spectroscopy, Structures, and Conformations of λ³-Cyclotriphosphazanes: Role of Negative Hyperconjugation

Ramaswamy Murugavel,† Setharampattu S. Krishnamurthy,*,† Jayaraman Chandrasekhar,‡ and Munirathinam Nethaji†

Departments of Inorganic and Physical Chemistry and Organic Chemistry, Indian Institute of Science, Bangalore-560 012, India

Received May 7, 1993®

The reactions of λ³-chlorocyclotriphosphazane $[EtNPCl]_3$ with phenols or trifluoroethanol yield the respective aryloxy- or trifluoroethoxy-containing λ³-cyclotriphosphazanes $[EtNP(OR)]_3$ (R = C_6H_4Br-4 (**2**), C_6H_5 (**3**), $C_6H_3Me_2$-3,5 (**4**), $C_6H_3Me_2$-2,6 (**5**), CH_2CF_3 (**6**)) as their *cis–trans* isomeric mixtures. The products have been characterized by IR and NMR spectroscopy. The crystal structures of both the *cis* (**2a**) and *trans* (**2b**) isomers of the *p*-bromophenoxy derivative have been determined by X-ray diffraction. Crystal data for **2a**: triclinic, $P\bar{1}$, a = 9.872(4) Å, b = 13.438(6) Å, c = 13.548(8) Å, α = 117.02(5)°, β = 96.00(6)°, γ = 105.38(4)°, Z = 2, final R = 0.080. Crystal data for **2b**: monoclinic, $P2_1/n$, a = 12.721(6) Å, b = 13.468(7) Å, c = 17.882(5) Å, β = 101.62(3)°, Z = 4, final R = 0.066. The *cis* isomer exhibits a chair-triaxial conformation and the *trans* isomer a boat-triaxial conformation. Conformational preferences of λ³-cyclotriphosphazanes have been probed by both MNDO and *ab initio* calculations on model systems $[HNPX]_3$ (X = H, F). In addition to vicinal lone pair repulsions, negative hyperconjugative interactions involving the nitrogen lone pairs and adjacent P–X σ* orbitals are found to be important (especially when X is an electronegative substituent) in determining the conformational preferences of λ³-cyclotriphosphazanes. The calculations also show that the axial → equatorial conversion at phosphorus has a large activation barrier in these systems.

Introduction

Whereas the chemistry of λ³-cyclodiphosphazanes is nearly a century old,[1] the first authentic examples of cyclotriphosphazanes were isolated only a decade ago. The cyclotriphosphazanes $[MeNPX]_3$ (X = Cl, Br) were obtained by Zeiss and Barlos[2] from the reaction of PX_3 and $MeN(SiMe_3)_2$, and subsequently, Keat and co-workers[3] obtained the λ³-cyclotriphosphazane $[EtNPCl]_3$ from the direct reaction of PCl_3 with ethylamine hydrochloride. Several halogen displacement reactions of the cyclotriphosphazane $[MeNPBr]_3$ have been carried out by Zeiss and co-workers.[4] Very little is known on the conformations of the six-membered ring in λ³-cyclotriphosphazanes.[5] Conformational analysis of several inorganic ring systems is of great importance because of their peculiarities as compared to carbocyclic systems.[6] Furthermore, the presence of three tricoordinate phosphorus centers in λ³-cyclotriphosphazanes would make them interesting ligands.[7]

Herein we report the synthesis and spectral characterization of a series of aryloxy- and trifluoroethoxy-containing λ³-cyclotriphosphazanes derived from $[EtNPCl]_3$. The structures of both the *cis* and *trans* isomers of a λ³-cyclotriphosphazane, *viz.* $[EtNP(OC_6H_4Br\text{-}4)]_3$, have been determined by single-crystal X-ray diffraction. Semiempirical MNDO and *ab initio* calculations on model ring systems $[HNPX]_3$ (X = H, F) have been carried out to probe into the electronic origin of the observed structural and conformational preferences.

Results and Discussion

Synthesis of Alkoxy- and (Aryloxy)cyclotriphosphazanes. Treatment of the *cis–trans* isomeric mixture of $[EtNPCl]_3$ (**1**) with phenols in the presence of diazabicyclooctane (DABCO) as an HCl acceptor yields the derivatives $[EtNP(OR)]_3$ (**2–5**). Reaction of $[EtNPCl]_3$ with $NaOCH_2CF_3$ in THF gives a 1:1 *cis–trans* isomeric mixture of $[EtNP(OCH_2CF_3)]_3$ (**6**). Compounds **2–5** have also been prepared by using the sodium salts

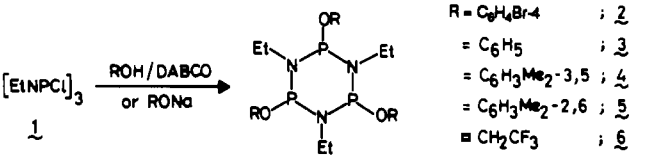

of the phenols. The use of triethylamine as the HCl acceptor in these reactions results in the formation of small amounts of cyclotriphosphazane oxides as well as some uncharacterizable products. On the other hand, when sodium aryloxide salts are used, the yield of side products is considerably reduced but the yield of the (aryloxy)cyclotriphosphazanes is also appreciably lowered.

Compounds **2–4** and **6** are isolated as their *cis–trans* isomeric mixtures. In contrast, the reaction with 2,6-dimethylphenol yields only the *trans* isomer of **5**. This difference is probably due to the bulkiness of the aryl group in **5**. The isomeric ratios of the products obtained are listed in Table I. The new cyclotriphosphazanes are characterized by elemental analyses and IR and ^1H, ^{13}C, and ^{31}P NMR spectroscopy. The *cis* and *trans* isomers of the *p*-bromophenoxy derivative (**2**) can be conveniently separated by fractional crystallization. From the oily isomeric mixture of **6**, the *cis* isomer **6a** slowly crystallizes over a period of 2–3 days at room temperature. The *trans* isomer **6b** could not be isolated in a pure state.

† Department of Inorganic and Physical Chemistry.
‡ Department of Organic Chemistry.
• Abstract published in *Advance ACS Abstracts,* October 15, 1993.

(1) Michaelies, A.; Schroeter, F. *Chem. Ber.* **1894**, *27*, 490.
(2) Zeiss, W.; Barlos, K. *Z. Naturforsch.* **1979**, *B34*, 423.
(3) Harvey, D. A.; Keat, R.; Rycroft, D. S. *J. Chem. Soc., Dalton Trans.* **1983**, 425.
(4) Zeiss, W.; Pointner, A.; Engelhardt, C.; Klehr, H. *Z. Anorg. Allg. Chem,* **1981**, *475*, 256.
(5) Prior to this study, there is only one brief report concerning the crystal structure of *cis*-$[MeNP(OC_6H_4Br\text{-}4)]_3$, but no details are available (Hess, H.; Zeiss, W. Unpublished results quoted in ref 4).
(6) Keat, R. *Top. Curr. Chem.* **1982**, *102*, 89.
(7) Murugavel, R.; Krishnamurthy, S. S.; Nethaji, M. *J. Chem. Soc., Dalton Trans.*, in press.

0020-1669/93/1332-5447$04.00/0

Table I. Isomeric Compositions of Aryloxy- and Alkoxy-Containing λ^3-Cyclotriphosphazanes $[EtNPX]_3$[a]

–X group	mp (°C)	yield (%)	isomer ratio *cis*:*trans*
Cl (**1**)	25–30	45	1:6
OC_6H_4Br-4 (**2**): *cis*, *trans*	97–99, 79–80	24, 53	1:2.2
OC_6H_5 (**3**)	oil	70	1:3.5
$OC_6H_3Me_2$-3,5 (**4**)	oil	76	1:2.5
$OC_6H_3Me_2$-2,6 (**5**)	79–81	64	0:1
OCH_2CF_3 (**6**): *cis*, *trans*	77–81, oil	25, 25	1:1

[a] Determined from ^{31}P NMR spectra at ≈25 °C.

Table II. Phosphorus-31 Chemical Shifts[a] for λ^3-Cyclotriphosphazanes $[EtNPX]_3$

–OR group	*cis* δ	*trans* δ_A	*trans* δ_X	*trans* $J(AX)$ (Hz)
Cl (**1**)	104.0	135.5	129.7	6.8
OC_6H_4Br-4 (**2**)	96.8	121.5	118.0	9.5
OC_6H_5 (**3**)	97.6	120.2	112.7	11.5
$OC_6H_3Me_2$-3,5 (**4**)	97.1	119.6	117.3	11.1
$OC_6H_3Me_2$-2,6 (**5**)		117.2	116.0	11.0
OCH_2CF_3 (**6**)	93.6	114.2	106.4	11.7

[a] In ppm relative to 85% H_3PO_4.

Spectral Characterization. The ^{31}P NMR data for cyclotriphosphazanes **2–6** are listed in Table II. The observed chemical shifts and coupling constants are comparable to those reported for the analogous *N*-methylcyclotriphosphazanes $[MeNP(OR)]_3$.[4] The ^{31}P NMR spectrum of the *cis* isomer gives a single peak around δ 100 ppm. The chemical shifts of the *cis*-alkoxy- and (aryloxy)cyclotriphosphazanes are shifted by 5–10 ppm downfield compared to the chloro compound. The ^{31}P NMR spectra of the *trans* isomers are of the A_2X type indicating the presence of two different kinds of phosphorus nuclei in the molecule. The spectra of the *trans* isomers of **2–5** are well resolved at room temperature. On the other hand, the spectrum of the *trans* isomer of the trifluoroethoxy derivative **6** shows broad peaks which are resolved at 233 K to give a doublet and a triplet. On lowering the temperature below 233 K, the doublet and the triplet collapse to two singlets, and on further cooling, these singlets are broadened. Besides, there is a noticeable change (≈4 ppm upfield) in the ^{31}P chemical shifts. The nature of the dynamic process causing these changes is not clear.

As in the case of cyclodiphosphazanes, the chemical shift of the *trans* isomer lies downfield from that of the *cis* isomer. However, the difference between ^{31}P chemical shifts for the *cis* and *trans* isomers of λ^3-cyclotriphosphazanes is less than 20 ppm (Table II) in contrast to the much larger difference (50–90 ppm) observed between *cis*- and *trans*-λ^3-cyclodiphosphazanes.[6] The two-bond PNP coupling constants $^2J(PP)$ for these compounds are in the range 9–11 Hz. These are only slightly different from the value observed for the parent cyclotriphosphazane, $[EtNPCl]_3$ (7 Hz).

The ^1H NMR spectra of the *cis* isomers (**2a–4a, 6a**) show the presence of only one type of –N*Et* group in the molecule whereas the spectra of the *trans* isomers (**2b–4b, 5, 6b**) display two resonances for the $-NCH_2CH_3$ protons. For **5**, two resonances are observed for the $-CH_3$ protons attached to the phenyl ring.

As in its ^1H NMR spectrum, the carbon-13 spectrum of the *cis*-isomer **2a** displays resonances for only one type of –NEt group; the methyl carbon of **2a** resonates as a singlet at δ 20.4, and the methylene carbons resonate as a triplet at δ 49.7 with a $^3J(PC)$ of 44.5 Hz. The spectrum of the *trans* isomer **2b**, on the other hand, shows two sets of resonances for the –NEt groups. The two types of methyl carbons give rise to singlets at δ 19.4 and 21.3 (1:2), respectively. The peak at 44.5 ppm arises from the methylene carbon of the –NEt group attached to the two phosphorus atoms in the same environment ($^2J(PC)$ = 30 Hz). The other two methylene carbon nuclei resonate at δ 47.3 as a doublet of doublet ($^2J(PC)$ = 28.7 and 41.4 Hz) owing to coupling to phosphorus nuclei in different environments.

Oxidation Reactions of Cyclotriphosphazanes. Treatment of **2a** or **2b** with Me_3NO as the oxidizing agent in CH_2Cl_2 yields the respective *cis*- or *trans*-λ^5-trioxocyclotriphosphazanes $[EtNP(O)(OC_6H_4Br\text{-}4)]_3$ (**10a,b**) in high yields (>90%).[8] The NMR

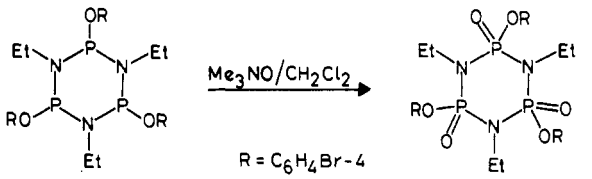

2a cis
2b trans
10a cis
10b trans

spectra of **10a,b** are very similar to those of their parent λ^3-cyclotriphosphazanes (**2a,b**). For compound **10a**, resonances due to only one type of –NEt group are observed in its ^1H and ^{13}C NMR spectra, while the spectra of **10b** show the presence of two sets of –NEt groups. The ^{31}P NMR spectrum of **10a** shows a single resonance at δ –1.8 ppm indicating the equivalence of all three phosphorus nuclei. The spectrum of the *trans* isomer **10b** shows an A_2X spectral pattern with a $^2J(PP)$ value of 24.7 Hz. From these NMR data and the crystal structures of λ^5-trioxocyclotriphosphazanes reported in the literature,[9a,11] one can conclude that the structures of **10a,b** would be similar to those of **2a,b** (see below); the oxo groups occupy the positions of the lone pairs in the parent λ^3-phosphorus compounds.

Structures of λ^3-Cyclotriphosphazanes. It has generally been assumed that the P_3N_3 ring in cyclotriphosphazanes will adopt a chair conformation and the ring nitrogen atoms will have a planar or a near-planar distribution of bonds.[6] This assumption is reasonable in view of the fact that the six-membered P_3N_3 ring fragments found in the cage compounds $P_4(NMe)_6$[12a] and its monosulfide[12b] and the methyl iodide adduct[12c] assume a chair conformation and the geometry around the ring nitrogen atoms in these compounds as well as in acyclic diphosphazanes,[13] cyclodiphosphazanes,[6] and cyclotetraphosphazanes[14] is trigonal-planar. However, a boat conformation for λ^3-cyclotriphosphazanes cannot be ruled out in view of the fact that the trioxo-λ^5-cyclotriphosphazanes are known to exhibit a boat or twist-boat conformation.[9a,11] Apart from the possible chair and boat conformations of the P_3N_3 rings, the exocyclic phosphorus substituents can have an axial or equatorial disposition with respect to the ring. Thus, there are four possible chair conformers and six possible boat conformers for λ^3-cyclotriphosphazanes as illustrated in Figure 1.

(8) The *N*-phenyl-λ^5-cyclotriphosphazane $[PhNP(O)Cl]_3$ has been prepared by Murray and co-workers by direct condensation reaction between $POCl_3$ and $PhNH_3Cl$.[9] The analogous *N*-alkyl compounds are not accessible by this route but are prepared by thermal or alkyl halide catalyzed rearrangement reactions of alkoxycyclotriphosphazenes.[10]

(9) (a) Johnson, O.; Murray, M.; Woodward, G. *J. Chem. Soc., Dalton Trans.* **1989**, 821. (b) Murray, M.; Woodward, G. *Phosphorus, Sulfur, Silicon* **1990**, *49/50*, 389.
(10) (a) Fitzsimmons, B. W.; Hewlett, C.; Shaw, R. A. *J. Chem. Soc.* **1964**, 4459. (b) Ferrar, W. T.; Distefano, F. V.; Allcock, H. R. *Macromolecules* **1980**, *13*, 158. (c) Dhathathreyan, K. S.; Krishnamurthy, S. S.; Vasudeva Murthy, A. R.; Shaw, R. A.; Woods, M. *J. Chem. Soc., Dalton Trans.* **1981**, 1928. (d) Karthikeyan, S.; Krishnamurthy, S. S. *J. Chem. Soc., Dalton Trans.* **1991**, 299.
(11) (a) Ansell, G. B.; Bullen, G. J. *J. Chem. Soc. A* **1968**, 3026. (b) Karthikeyan, S.; Vyas, K.; Krishnamurthy, S. S.; Cameron, T. S.; Vincent, B. R. *J. Chem. Soc., Dalton Trans.* **1988**, 1371.
(12) (a) Cotton, F. A.; Troup, J. M.; Casabianca, F.; Riess, J. G. *Inorg. Chim. Acta.* **1974**, *11*, L33. (b) Cotton, F. A.; Riess, J. G.; Rice, C. E.; Stults, B. R. *Inorg. Chem.* **1978**, *17*, 3521. (c) Hunt, G. W.; Cordes, A. W. *Inorg. Chem.* **1974**, *13*, 1688.
(13) Babu, R. P. K.; Krishnamurthy, S. S.; Nethaji, M. *Heteroatom Chem.* **1991**, *2*, 477.
(14) Gallicano, K. D.; Paddock, N. L.; Rettig, S. J.; Trotter, J. *Can. J. Chem.* **1982**, *60*, 2415.

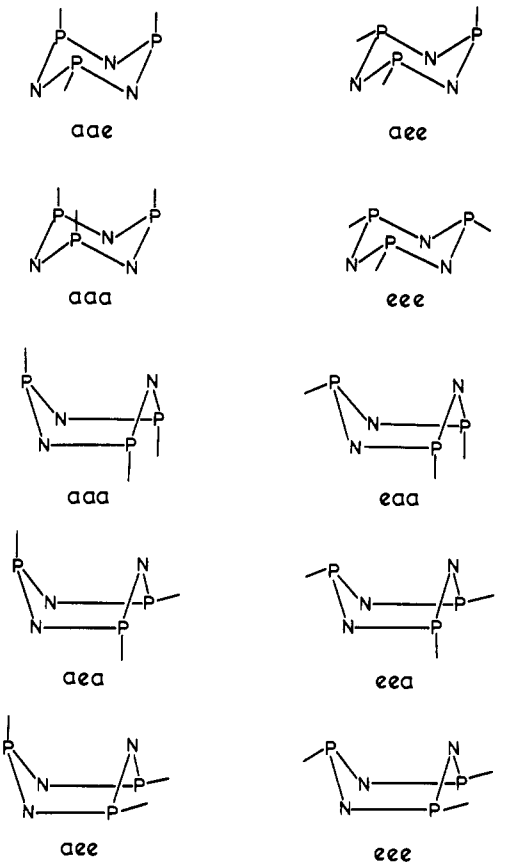

Figure 1. Various possible conformations for λ³-cyclotriphosphazanes (substituents on nitrogen atoms and lone pair omitted for clarity; a = axial, e = equatorial).

The identification of the preferred molecular shapes of cyclotriphosphazanes by NMR spectroscopy is difficult.[6] Phosphorus-31 NMR spectroscopy does not provide an unambiguous distinction between the *aaa* and *eee* conformations of the *cis* isomer in the chair form (both of which would be expected to give only a single-line spectrum). In the same way, the observed spectral behavior of the *trans* isomer could be fitted to either *aae* or *aee* dispositions in the chair conformation and also for the *aaa* or *eee* arrangements in the boat form. Out of these 10 possibilities, boat-*aea* and boat-*eea* conformers can be excluded as they would be expected to give an AMX pattern instead of the observed A_2X pattern.

In order to clearly establish the conformational preferences of cyclotriphosphazanes, single-crystal X-ray structural studies of both the *cis* and *trans* isomers of **2** have been carried out. In spite of the instability of the crystals toward air, moisture, and X-rays (see Experimental Section), it has been possible to obtain reasonably good structural parameters for both the isomers. The molecular structures of the *cis* and *trans* isomers **2a,b** are shown in Figure 2. The selected structural parameters are listed in Table III.

Both mean plane calculations and torsional angles are used to define the stereochemistry of the P_3N_3-phosphazane rings in these structures. Symmetries displayed by the torsional angles have been used to identify the conformations of six-membered rings in carbocyclic systems.[15] Three intersecting C_2 axes and three mirror planes are essential for the chair conformation, whereas the presence of two orthogonal mirror planes characterizes the boat conformation. However, in the ring systems formed by heteroatoms there may be deviations from the ideal conformations; the degree of departure from the ideal 2-fold symmetry (ΔC_2) and mirror symmetry (ΔC_s) will give an estimate of the distortion from any of the idealized conformations.[16] Torsional angles of the phosphazane rings in **2a,b** and the asymmetry parameters are

(15) Duax, W. L.; Weeks, C. M.; Rohrer, D. C. *Topics in Stereochemistry*; Allinger, N. L., Eliel, E. L., Eds.; John-Wiley: New York, 1976; Vol. IX, p 279.

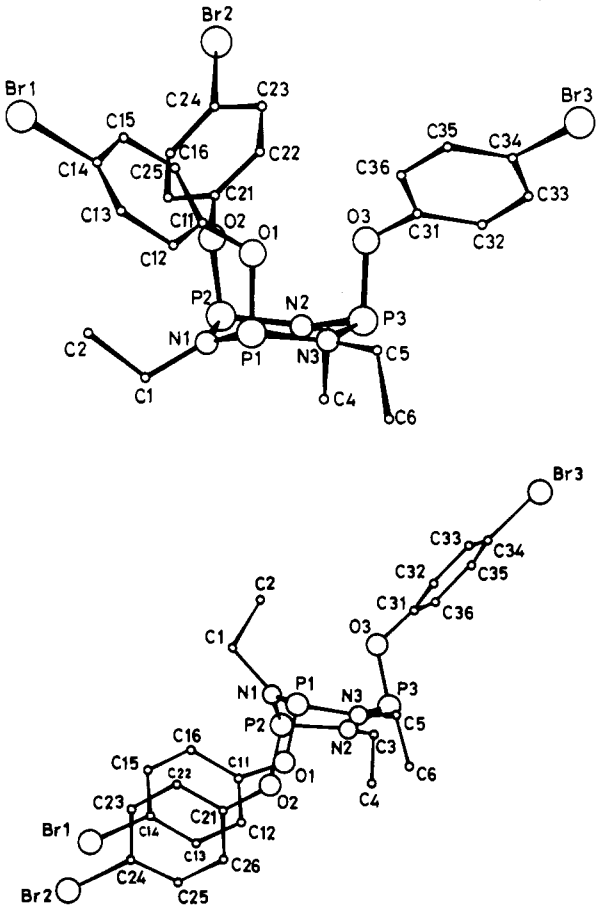

Figure 2. Molecular structures of (top) *cis*-[EtNP(OC_6H_4Br-4)]$_3$ (**2a**) and (bottom) *trans*-[EtNP(OC_6H_4Br-4)]$_3$ (**2b**).

Table III. Selected Structural Parameters (Å, deg) for *cis*- and *trans*-[EtNP(OC_6H_4Br-4]$_3$ (**2a,b**)

	2a	**2b**
P1–N1	1.68(1)	1.67(2)
N1–P2	1.69(2)	1.69(2)
P2–N2	1.67(1)	1.67(2)
N2–P3	1.68(1)	1.62(2)
P3–N3	1.68(2)	1.63(2)
N3–P1	1.69(1)	1.68(2)
P1–O1	1.67(1)	1.62(2)
P2–O2	1.65(1)	1.65(2)
P3–O3	1.67(1)	1.61(2)
N3–P1–O1	96.6(8)	96.2(8)
N1–P1–O1	103.8(8)	103.8(8)
N1–P1–N3	101.9(8)	99.0(9)
N1–P2–O2	96.6(7)	97.3(9)
N1–P2–N2	102.0(7)	103.9(8)
N2–P2–O2	103.4(8)	99.2(9)
N2–P3–O3	97.5(7)	100(1)
N2–P3–N3	101.2(8)	97(1)
N3–P3–O3	104.4(7)	100(1)
P1–N1–C1	116(1)	128.9(9)
P1–N1–P2	130(1)	115(1)
P2–N1–C1	114(1)	115(1)
P2–N2–C3	112(1)	133(1)
P2–N2–P3	134.4(9)	111(1)
P3–N2–C3	112(1)	111(2)
P1–N3–P3	133.9(9)	132(1)
P3–N3–C5	113(1)	114(1)
P1–N3–C5	110(1)	110(1)
P1–O1–C11	119(1)	122(1)
P2–O2–C21	119(1)	124(1)
P3–O3–C31	117(1)	123(2)

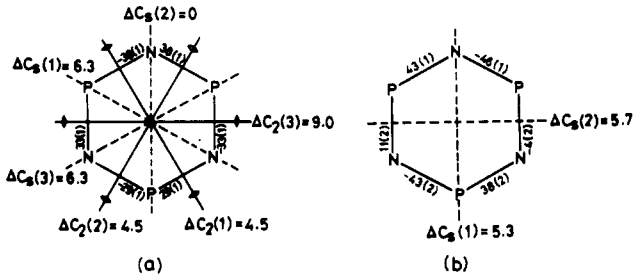

Figure 3. P_3N_3 ring dihedral angles and asymmetry paramaters (ΔC_2 and ΔC_s) for (a) *cis*-[EtNP(OC_6H_4Br-4)]$_3$ (**2a**) and (b) *trans*-[EtNP(OC_6H_4Br-4)]$_3$ (**2b**).

shown in Figure 3. The *cis* isomer **2a** exhibits a flattened chair conformation, and the *trans* isomer **2b** adopts a boat conformation. The small values of the asymmetry parameters indicate that the conformations of these rings do not deviate to an appreciable extent from an ideal chair or an ideal boat conformation, respectively. A notable feature of both the structures is that all the exocyclic phosphorus substituents occupy the axial positions.

The P–N bond lengths in **2a** vary from 1.67 to 1.69 Å with an average value of 1.68 Å. The P–N bond distances in the *trans* isomer, **2b** vary over a wide range (1.62–1.69 Å) with an average value of 1.66 Å. The lengths of the two P–N bonds about the unique phosphorus atom P3 are significantly shorter than the other four P–N bonds. The average P–N distances observed for both **2a** and **2b** are much shorter than the value normally accepted for a P–N single bond (1.75–1.80 Å) but comparable with the values found for cyclodiphosphazanes[6] indicating possible P–N multiple bond character in these molecules. The average P–O distance in **2a** is 1.66 Å, and that in **2b**, 1.63 Å. The bond angles around the ring nitrogen atoms in both **2a** and **2b** vary over a wide range (110.0–134.4° for **2a** and 110.0–128.9° for **2b**); the angles within the ring (mean 131° for *cis* and 133° for *trans*) are much larger than those involving the exocyclic carbon atoms (mean P–N–C angle for **2a,b** is 113°).[17] Neverthless the geometry around all the nitrogen atoms is planar (sum of angles close to 360°).

Electronic Factors Operating in λ^3-Cyclotriphosphazanes. The preference of the *cis* and *trans* isomers **2a,b** for triaxial chair and boat conformations can be rationalized on the basis of *the gauche effect*: In the energetically favorable conformation, the lone pair on each of the phosphorus atoms would avoid eclipsing interactions with adjacent nitrogen lone pairs.[18] On this basis, the *aaa* chair conformer for *cis*-**2a** would ideally have the favorable orthogonal orientation between the equatorial phosphorus lone pairs and vicinal nitrogen lone pairs. Similarly, the eclipsing interactions would be minimized in the boat triaxial conformer for the *trans* isomer. If this isomer were to adopt the chair conformation, the substituents at phosphorus would have to be placed in the *aae* or *aee* positions, leading to partial eclipsing interactions involving lone pairs.

While lone pair repulsions are no doubt important in these systems, the structural features such as short P–N distances imply the operation of additional electronic effects. In order to unravel these interactions, MO calculations have been performed on the model P_3N_3 ring systems [HNP(X)]$_3$ (X = H (**7**), F (**8**)). The simple system, **7**, was chosen to determine the conformational effects resulting essentially from adjacent lone pair interactions.

(16) Asymmetry parameters ΔC_2 and ΔC_s were calculated from the equations given in ref 15.
(17) The bond angles around the ring phosphorus atoms in the *cis* isomer vary from 96.6 to 104.4°, and the corresponding values for the *trans* isomer vary from 96.2 to 103.9°. The average N–P–N angles in **2a,b** are 101.7 and 99.7°, respectively. These values are much larger than the small ring N–P–N angles found for cyclodiphosphazanes (≈80.0°).[6]
(18) Wolfe, S. *Acc. Chem. Res.* **1975**, *5*, 103.

Table IV. Results of *ab Initio* Calculations on [XPNH]$_3$ (**7**, **8**)

	3-21G		3-21G(*)	
conformer	rel energy (kcal/mol)	dipole mom. (Debye)	rel energy (kcal/mol)	dipole mom. (Debye)
	X = H (**7**)			
chair; *aaa*-**7a**	0.0[a]	1.1	0.0[b]	1.2
chair; *aae*-**7b**	13.7	2.5	13.5	2.7
chair; *aee*-**7c**	32.5	2.8	32.4	3.0
chair; *eee*-**7d**	48.3	3.3	48.1	3.5
boat; *aaa*-**7e**	9.7	0.7	9.6	0.7
	X = F (**8**)			
chair; *aaa*-**8a**	0.0[c]	5.2	0.0[d]	4.1
chair; *aae*-**8b**	9.9	2.9	10.6	2.7
chair; *aee*-**8c**	23.4	3.1	23.3	1.2
chair; *eee*-**8d**	36.6	3.5	35.8	0.4
boat; *aaa*-**8e**	0.0	1.5	1.1	1.1

[a] Total energy: −1182.897 97 Hartree. [b] Total energy: −1183.287 19 Hartree. [c] Total energy: −1478.014 66 Hartree. [d] Total energy: −1478.448 00 Hartree.

The fluoro derivative, **8**, was examined to assess the additional interactions resulting from electronegative substituents.[19]

For each model, the four possible chair conformations and the six possible boat conformations were initially studied at the MNDO level (Figure 1).[20,21] The chair triaxial conformer was indeed predicted to be the most stable form for both **7** and **8**. However, the conformational energy differences were generally too small. The largest energy differences among the 10 conformers were only 5.4 and 6.7 kcal/mol, respectively, for **7** and **8**. Our variable-temperature NMR studies on pure *cis* and *trans* isomers of [EtNP(OC_6H_4Br-*4*)]$_3$ (**2a,b**) do not provide any evidence for the presence of multiple conformers in the range −100 to 100 °C. A previous theoretical study on a related system [NSX]$_3$ also revealed smaller conformational energy differences at the MNDO level compared to *ab initio* calculations.[22] We therefore calculated the conformational energetics associated with **7** and **8** at the *ab initio* level.[23]

The energies of the four chair conformers and the triaxial boat conformer for **7** and **8** were obtained with the 3-21G and 3-21G(*) basis sets (Table IV).[24] At both levels, the chair triaxial forms **7a** and **8a** are clearly favored for the *cis* isomer and the boat triaxial form **7e** and **8e** for the *trans* isomer. The alternative conformers considered are much higher in energy and are unlikely to be populated to any significant extent under ambient conditions. The most stable *cis* and *trans* isomers of **7** differ in energy by 9.6 kcal/mol. This result is consistent with the importance of lone pair repulsions; residual eclipsing interactions cannot be avoided in the boat form **7e** relative to the ideal alignment of lone pairs in **7a**. Interestingly, the corresponding conformers are isoenergetic in the fluoro derivatives (Table IV). Intramolecular dipole repulsions involving the triaxial P–F bonds presumably destabilize the chair form relative to the boat conformer. The computed dipole moments support this interpretation. While the values do

(19) The hydroxy derivative [HNP(OH)$_3$] would have been a more appropriate model for the aryloxy derivatives **2a,b**, for which X-ray crystal structures have been determined. However, the conformational flexibility about the P–O bond introduces some uncertainties in the calculations. Therefore, to keep the electronic interpretation unambiguous, computations were confined to the hydrido and fluoro derivatives (**7** and **8**).
(20) The molecular geometries of all the 10 conformers were fully optimized without imposing any molecular symmetry. Optimized structures and energies are provided as supplementary material.
(21) MOPAC program was used; see: Stewart, J. J. P. *J. Comput.-Aided Mol. Des.* **1990**, *4*, 1.
(22) Jandas-Prezel, E.; Maggiulli, R.; Mews, R.; Oberhammer, H.; Stohrer, W. D. *Chem. Ber.* **1990**, *123*, 2177.
(23) The MNDO optimized geometries were used. It is known from earlier studies on negative hyperconjugation in sugars (the anomeric effect) that the MNDO geometries are quite reliable, although the conformational energetics are underestimated. See: Woods, R. J.; Szark, W. A.; Smith, V. H. *J. Chem. Soc., Chem. Commun.* **1991**, 334.
(24) Hehre, W. J.; Radom, L.; Schleyer, P. v. R.; Pople J. A. *Ab initio Molecular Orbital Theory*; Wiley: New York, 1986.

Table V. Calculated H–N–P–X (X = H, F) Torsional Angles (deg) of **7** and **8** and the Corresponding C–N–P–O Angles (deg) in **2a,b**

conformer	H10–N2–P1–X7	H10–N2–P3–X8	H11–N4–P3–X8	H11–N4–P5–X9	H12–N6–P1–X7	H12–N6–P5–X9
chair; *aaa*						
X = H, **7a**	−131.3	129.0	−126.7	128.0	130.0	−126.7
X = F, **8a**	−104.4	108.2	−109.3	106.9	101.6	−102.9
X = O, **2a** (expt)	−116.3	110.9	−101.4	90.5	88.9	−88.6
chair; *aae*						
X = H, **7b**	13.6	128.6	−126.9	129.3	−15.0	−129.8
X = F, **8b**	46.9	105.1	−110.1	107.3	−52.2	−97.4
chair; *aee*						
X = H, **7c**	45.7	−54.2	35.2	123.1	−7.8	140.7
X = F, **8c**	53.4	−55.4	47.3	104.2	−41.6	−108.2
chair; *eee*						
X = H, **7d**	33.7	−51.1	65.2	−55.9	0.6	9.0
X = F, **8d**	41.8	−53.2	66.7	−61.9	−32.3	39.2
boat; *aaa*						
X = H, **7e**	−122.9	−61.7	128.3	−133.1	119.7	69.1
X = F, **8e**	−106.1	−67.8	113.6	−118.3	99.5	78.8
X = O, **2b** (expt)	−86.3	−101.6	123.4	−125.3	99.7	88.2

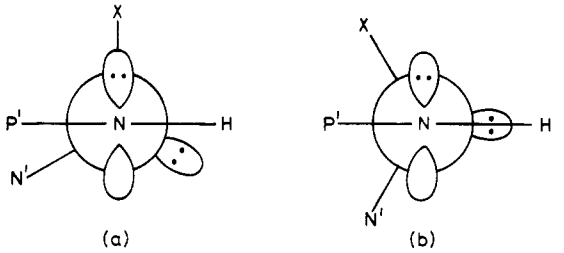

Figure 4. Ideal conformations of P'NH–PXN' units for (a) maximizing negative hyperconjugation and (b) minimizing lone pair repulsions.

not differ significantly for **7a** and **7e**, the calculated dipole moment is reduced from 4.1 to 1.1 D on going from **8a** to **8e**.

In addition to lone pair interactions and dipole repulsions, potential multiple bonding effects are also evident from the observed P–N distances in **2a,b**. However, phosphorus d orbitals are probably unimportant in λ³-phosphazanes, as reflected in the negligible change in the computed energetics of **7** and **8** at the 3-21G and 3-21G(*) levels. Multiple bonding effects in compounds of phosphorus and many other main group elements can be explained by invoking an alternative model based on negative hyperconjugation.[25] This stabilizing effect arises from the interaction of the nitrogen lone pair with the adjacent P–X σ* orbitals. For these interactions to be most effective, the nitrogen lone pair (lp) must have a periplanar relationship with the P–X bond, *i.e.* the lp–N–P–X dihedral angle should be 0 or 180° (Figure 4a). In this orientation, the nitrogen and phosphorus lone pairs are not mutually orthogonal. Due to pyramidality of the phosphorus, the lp–N–P–lp dihedral angles will be closer to 60 or 120°. Hence, negative hyperconjugation and lp–lp repulsions place conflicting requirements on the preferred dihedral angles. In terms of the H–N–P–X dihedral angles, a value of 90° is preferred for maximum negative hyperconjugative stabilization (Figure 4a), while a value closer to 120° is appropriate to have the least lp–lp repulsions (Figure 4b).

Table V lists the H–N–P–X dihedral angles of interest for the calculated structures of **7** and **8**. For an experimental comparison, the C–N–P–O dihedral angles of both the *cis* and *trans* isomers of $[EtNP(OC_6H_4Br\text{-}4)]_3$ (**2a,b**) have been included.

The H–N–P–H dihedral angles of the *cis*-chair-triaxial isomer **7a** is close to 120°, indicating that the geometry of this isomer is mainly dictated by the minimization of the adjacent lp–lp repulsions. More strikingly, as we move from hydrogen to fluorine, the H–N–P–F dihedral angles in **8a** are significantly shorter than 120° tending toward 90°, the ideal value for negative hyperconjugative interactions. These negative hyperconjugative interactions stabilize the molecule to a greater extent in the case of more electronegative substituents as a result of an increased coefficient at phosphorus and lowering of the energy of the P–X σ* orbital. Interestingly, the C–N–P–X angles in the *cis*-chair-triaxial form **2a** approach the value of 90° reflecting the role of negative hyperconjugative interactions. A similar trend is seen in the dihedral angles of *trans*-boat-triaxial conformations of both **7** and **8** and **2b**. In the case of the *trans*-boat-triaxial conformation **7e** the H–N–P–H dihedral angles are close to 120° around the unique nitrogen atom and the values of 60 and 120° around the other two nitrogen atoms. In **8e** and **2b** the corresponding dihedral angles move closer to 90°, maximizing negative hyperconjugative interactions. The H–N–P–X dihedral angles of the alternative conformers **7b–d** and **8b–d** suggest that these arrangements are unfavorable for negative hyperconjugative interactions and entail destabilizing adjacent lp–lp repulsions. Hence, the corresponding forms are not experimentally observed for **2**.

In addition to the reduced stability of the isomers with equatorial substituents, the calculations also reveal a large activation barrier for the axial → equatorial conversion process. Estimates of the barrier for the inversion process were obtained from *ab initio* calculations at the 3-21G level on the N–P–N ring fragments $XP(NH_2)_2$ (X = H, OH, F (**9**)) with C_s symmetry constraints.[26]

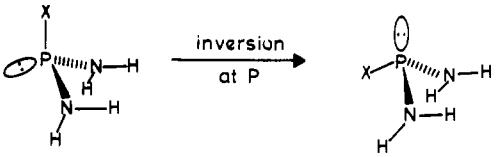

X = H ; **9a**
= OH ; **9b**
= F ; **9c**

A single minimum with dihedral angles corresponding to a pseudo-axial fragment was obtained in each case. The inversion barriers for **9a–c** were estimated to be 59.9, 107.7, and 126.3 kcal/mol, respectively. The barriers are quite large for electronegative

(25) (a) Lehn, J. M.; Wipff, G. *J. Chem. Soc., Chem. Commun.* **1975**, 800. (b) Biddlestone, M.; Keat, R.; Parkes, H. G.; Rose, H.; Rycroft, D. S.; Shaw, R. A. *Phosphorus, Sulfur* **1985**, *25*, 25. (c) Reed, A. E.; Schleyer, P. v. R. *J. Am. Chem. Soc.* **1990**, *112*, 1434. (d) Schleyer, P. v. R.; Kos, A. *Tetrahedron* **1983**, *39*, 1141. (e) Korkin, A. A. *Russ. Chem. Rev. (Engl. Transl.)* **1992**, *61*, 473.

(26) The total energies computed for the stable pseudo-axial forms **9a–c** are −450.187 72, −524.664 73, and −548.358 52 Hartree, respectively. Analytical vibrational frequencies for **9a,c** yielded a Hessian of zero confirming that the structures were true minima. In the case of **9b** an imaginary frequency for O–H torsion was obtained. Neverthless, the structure represents a suitable model for the system represented by **2**. In all the cases, the pseudo-equatorial structure rearranges by N–H torsional modes to the pseudo-axial form on geometry optimization, a process not possible in the ring systems. Hence the energetics of axial → equatorial conversion was estimated by varying the X–N–P–N' dihedral angles in increments of 10° while keeping the rest of geometry constant.

substituents (X). This explains the stability of the triaxial forms **2a,b**, which do not convert into equatorial forms even on heating to 100 °C for several hours.

Conclusion

Structural data for λ^3-cyclotriphosphazanes and theoretical studies presented in this paper throw light on the conformational preferences of the six-membered P_3N_3 rings. The observed conformations are a compromise between minimizing the P–N lone pair and electrostatic dipolar repulsions and maximizing negative hyperconjugative interactions.

Experimental Section

Apparatus and Chemicals. All experimental manipulations were performed under an atmosphere of dry nitrogen in a vacuum system or using Schlenk apparatus. Petroleum ether (60–80 °C), benzene, dichloromethane, chloroform, tetrahydrofuran, and 1,1,2,2-tetrachloroethane were purified by conventional procedures[27] and freshly distilled prior to use. Ethylamine hydrochloride (Fluka) was dried in a vacuum desiccator over anhydrous $CaCl_2$ for 12 h prior to use. PCl_3, 2,6-dimethylphenol, 3,5-dimethylphenol, and trifluoroethanol (all Fluka), trimethylamine *N*-oxide (TMNO) (Sigma), and 4-bromophenol and diazabicyclooctane (both E-Merck) were used as purchased. The ^1H, ^{13}C (for both Me_4Si internal standard), ^{19}F ($CFCl_3$ external standard), and ^{31}P (85% H_3PO_4 external standard) NMR spectra were obtained from a Bruker ACF 200 or a Bruker AMX-400 spectrometer. Chemical shifts downfield from the standard are assigned positive values. Infrared spectra were recorded using a Bio-Rad FTIR or a Perkin-Elmer Model 457 spectrometer. The mass spectrum of **6a** was recorded on a JEOL JMS-DX-303 spectrometer fitted with a JMA DA-5000 data system. Microanalyses were performed on an Heraeus CHN-O-Rapid elemental analyzer. Melting points were determined on a Reichert-Kofler microheating stage fitted with a polarizing microscope and were uncorrected.

The parent cyclotriphosphazane $[EtNPCl]_3$ was prepared by the reaction between $EtNH_2{\cdot}HCl$ and PCl_3 in boiling 1,1,2,2-tetrachloroethane following the procedure of Keat and co-workers.[28] (*Caution*! $[EtNPCl]_3$ is a highly reactive compound and catches fire when exposed to moist air or brought in contact with water. For the precautions to be taken during the synthesis of this compound, see ref 28.)

Preparation of $[EtNP(OC_6H_4Br\text{-}4)]_3$ (2). To a stirred solution of 4-bromophenol (4.5 g, 26 mmol) and diazabicyclooctane (1.5 g, 13.3 mmol) in benzene (100 mL), was added $[EtNPCl]_3$ (2.75 g, 8.4 mmol) in drops at 0 °C. The reaction mixture was slowly brought to room temperature, stirred for 2 h, and boiled under reflux for a further 12 h. The reaction mixture was cooled; diazabicyclooctane hydrochloride was filtered off and solvent removed from the filtrate *in vacuo* to yield a viscous oil. This oil was passed through a silica gel column using petroleum ether–benzene (3/1) mixture as eluent to remove any unreacted phenol or diazabicyclooctane. The resulting highly viscous oil contained a mixture of both the *cis* and *trans* isomers of $[EtNP(OC_6H_4Br\text{-}4)]_3$ (**2a,b**).

The isomers were separated by dissolving the oil in a minimum quantity of hot petroleum ether (20–25 mL). Slow cooling of the mixture deposited crystals of the *cis* isomer **2a** over a period of 24 h. At this point, the ^{31}P NMR spectrum of the mother liquor showed that it was almost free of this isomer. Crystals of **2a** were separated by filtration and washed with a minimum of cold petroleum ether. The filtrate was concentrated and cooled to 0 °C to get crystals of **2b** (yields based on $[EtNPCl]_3$: **2a**, 24%; **2b**, 53%).

Analytical and Spectroscopic Data for *cis*-$[EtNP(OC_6H_4Br\text{-}4)]_3$ (2a). Mp: 97–99 °C. CHN analysis [found (calcd)]: C, 38.9 (39.0); H, 3.7 (3.7); N, 5.9 (5.7). IR (Nujol): 1584, 1380, 1324, 1161, 1065, 1008, 831, 726, and 687 cm^{-1}. ^1H NMR ($CDCl_3$): δ 1.05 (CH_3, t, $^3J_{HH}$ = 7.1 Hz), 3.38 (CH_2, q of t, $^3J_{PH}$ = 11.3 Hz, $^3J_{HH}$ = 7.1 Hz), 6.8–7.3 (phenyl protons, AA′BB′ pattern). $^{31}P\{^1H\}$ NMR (CH_2Cl_2): δ 96.8 (s). ^{13}C NMR (CH_2Cl_2): δ 20.4 (CH_3, s), 49.7 (CH_2, t, $^3J_{PC}$ = 44.5 Hz), carbon nuclei of the aryl rings at δ 117.4, 124.4, 134.6, and 156.2.

***trans*-$[EtNP(OC_6H_4Br\text{-}4)]_3$ (2b).** Mp: 79–80 °C. Analytical data [found (calcd)]: C, 38.8 (39.0); H, 3.6 (3.7); N, 6.1 (5.7). IR (Nujol): 1582, 1482, 1460, 1377, 1222, 1166, 1066, 937, 849, and 729 cm^{-1}. ^1H NMR ($CDCl_3$): δ 1.09 (CH_3, 3H, t, $^3J_{HH}$ = 7.0 Hz), 1.18 (CH_3, 6H, t, $^3J_{HH}$ = 7.0 Hz), 3.1–3.5 (CH_2, complex multiplet pattern), 6.7–7.3 (aryl protons). $^{31}P\{^1H\}$ NMR (CH_2Cl_2): A_2X pattern, δ 121.5 (d, $^2J_{PP}$ = 9.4 Hz), 118.0 (t). ^{13}C NMR (CH_2Cl_2): δ 19.4 (CH_3, 1C), 21.3 (CH_3, 2C), 44.5 (CH_2, 1C, t, $^2J_{PC}$ = 30 Hz), 47.3 (CH_2, 2C, d of d, $^2J_{PC}$ = 28.7, 41.4 Hz), carbon nuclei of the aryl ring at δ 118.0, 125.0, 125.1, 135.1, and 156.4.

The phenoxy and 3,5-methylphenoxy and 2,6-dimethylphenoxy derivatives were prepared in the same way as described above. In the first two instances, the isomeric mixtures of the cyclotriphosphazanes could not be separated.

$[EtNP(OPh)]_3$ (3): Viscous oil; yield 70% based on $[EtNPCl]_3$. Isomer *cis*/*trans* ratio: 1:3.5. ^{31}P NMR (CH_2Cl_2): *cis* δ 97.6, *trans* δ 120.2 (d, 2P), 118.0 (t, 1P, $^2J_{AX}$ = 11.5 Hz). ^1H NMR resonances of *cis* and *trans* isomers could not be separately assigned. However, the integrated intensities were consistent with the formula of the compound.

$[EtNP(OC_6H_3Me_2\text{-}3,5)]_3$ (4): Viscous oil; yield 76% based on $[EtNPCl]_3$. Isomer *cis*/*trans* ratio: 1:2.2. ^{31}P NMR (CH_2Cl_2): *cis* δ 97.1, *trans* δ 119.6 (d, 2P), 117.3 (t, 1P, $^2J_{AX}$ = 11.1 Hz). ^1H NMR resonances of *cis* and *trans* isomers could not be separately assigned. However, the integrated intensities were consistent with the formula of the compound.

$[EtNP(OC_6H_3Me_2\text{-}2,6)]_3$ (5). The 2,6-dimethylphenoxy derivative was formed only as the *trans* isomer and purified by column chromatography over silica gel: Yield 64% based on $[EtNPCl]_3$; mp 79–81 °C. Anal. Found (calcd): C, 61.3 (61.5); H, 7.0 (7.2); N, 7.3 (7.2). IR (Nujol): 1593 (s), 1464 (s), 1380 (s), 1311 (m), 1263 (s), 1185 (s), 1161 (vs), 1089 (s), 1056 (s), 927 (vs), 823 (vs), 762 (s), 747 (s), 717 (s), 669 (m), 639 (w) cm^{-1}. ^1H NMR ($CDCl_3$): δ 1.03 (t, 6H, CH_3, $^3J_{HH}$ = 7 Hz), 1.18 (t, 3H, CH_3, $^3J_{HH}$ = 7 Hz), 2.37 (s, 6H, CH_3-aryl), 2.42 (s, 12H, CH_3-aryl), 3.2–3.6 (multiplet, 6H, CH_2), 6.8–7.0 (multiplet, 9H, aryl protons). ^{31}P NMR (CH_2Cl_2): δ 117.2 (d, 2P), 116.0 (t, 1P, $^2J_{AX}$ = 11.1 Hz).

Preparation of $[EtNP(OCH_2CF_3)]_3$ (6). A solution of $[EtNPCl]_3$ (1 g, 1 mmol) in benzene (10 mL) was added dropwise to a solution of sodium trifluoroethoxide [prepared from trifluoroethanol (0.9 g, 3 mmol) and sodium (0.21 g, 3 mmol) in THF (50 mL)]. The reaction mixture was stirred for 24 h and filtered to remove NaCl. Solvent was removed from the filtrate under reduced pressure to yield a 1:1 *cis*/*trans* isomeric mixture of **6a,b** in 50% yield. The product was a free flowing oil; it was purified by column chromatography over silica gel. The *cis* isomer **6a** slowly crystallized from the oil over a period of 2 days. Mp of **6a**: 77–81 °C. Spectroscopic data for **6a**: ^1H NMR ($CDCl_3$) δ 1.21 (t, CH_3, $^3J_{HH}$ = 7 Hz), 3.42 (q of t, $-NCH_2$, $^3J_{PH}$ = 17.8 Hz, $^3J_{HH}$ = 7 Hz), 4.00 (m, $-OCH_2$); ^{19}F NMR ($CDCl_3$) δ −12.4 (s); ^{31}P NMR (CH_2Cl_2) at 298 K δ 94.7: ^{31}P NMR (CH_2Cl_2) at 233 K δ 93.6 (s). Data for **6b**: ^{31}P NMR (CH_2Cl_2) at 298 K δ 111.4 (s, 1P), 117.6 (s, 2P); ^{31}P NMR (CH_2Cl_2) at 233 K δ 106.4 (t, 1P, $^2J_{AX}$ = 11.7 Hz), 114.2 (d, 2P). MS for **6a**: *m*/*e* 519 (M^+), 490 (base peak, $M^+ - Et$).

Reaction of 2a with TMNO. The *cis* isomer **2a** (0.79 g, 1 mmol) was stirred with a 5-fold excess of TMNO (0.38 g, 5 mmol) in CH_2Cl_2 (25 mL) for 72 h at room temperature, and the solvent was removed *in vacuo* to give *cis*-$[EtNP(O)(OC_6H_4Br\text{-}4)]_3$ (**10a**) in almost quantitative yield. The product was recrystallized from 1:3 CH_2Cl_2/petroleum ether solution. Mp: 183 °C. Anal. Found (calcd): C, 35.7 (35.7); H, 3.6 (3.5); N, 5.6 (5.4). $^{31}P\{^1H\}$ NMR (CH_2Cl_2): δ −1.8.

Reaction of 2b with TMNO. The *trans* isomer **2b** (0.79 g, 1 mmol) was dissolved in CH_2Cl_2 (25 mL), and the solution was stirred with a 5-fold excess of TMNO (0.38 g, 5 mmol) for 72 h at room temperature. Solvent was removed *in vacuo* to give *trans*-$[EtNP(O)(OC_6H_4Br\text{-}4)]_3$ (**10b**) in *ca.* 95% yield. The product was recrystallized from 1:3 CH_2Cl_2/petroleum ether solution. Mp: 195 °C. Anal. Found (calcd): C, 35.6 (35.7); H, 3.6 (3.5); N, 5.5 (5.4). ^1H NMR ($CDCl_3$): δ 1.21 (t, CH_3, 3H, $^3J_{HH}$ = 7 Hz), 1.26 (t, CH_3, 6H, $^3J_{HH}$ = 7 Hz), 3.51-3.64 (multiplet, 2H, CH_2), 3.65–3.82 (multiplet, CH_2, 4H), 6.94–7.54 (multiplet, 9H, aromatic resonances). ^{13}C NMR ($CDCl_3$): δ 16.6 (s, 2C, CH_3), 17.4 (s, 1C, CH_3), 42.3 (s, 2C, CH_2), 43.9 (s, 1C, CH_2), 118.7, 119.27, 119.28, 121.9, 122.0, 123.4, 123.5, 132.9, 133.0, 148.6, 148.7, 149.2 (aromatic resonances). $^{31}P\{^1H\}$ NMR ($CDCl_3$): A_2X pattern, δ_A −0.7 (d, 2P, $^2J_{PP}$ = 24.7 Hz), δ_X 2.5 (t, 1P).

X-ray Structures of *cis*- and *trans*-$[EtNP(OC_6H_4Br\text{-}4)]_3$ (2a,b). The crystals were obtained as rectangular plates, and a suitable crystal of each isomer was encapsulated in a Lindermann capillary as the crystals were found to be sensitive to air and moisture. Each crystal was centered on an Enraf-Nonius CAD-4 automated four-circle diffractometer equipped with a Mo Kα source (graphite monochromator). A total of 25 well-dispersed high-angle reflections were accurately measured, and the lattice parameters as well as crystal orientation were optimized by

(27) Perrin, D. D.; Armargeo, W. L. F. *Purification of Laboratory Chemicals*, 3rd Ed.; Pergamon Press: London, 1988.
(28) Gemmill, J.; Keat, R. *Inorg. Synth.* **1988**, *25*, 13.

Table VI. Crystal Data for *cis*- and *trans*-[EtNP(OC$_6$H$_4$Br-4)]$_3$

	2a	**2b**
chem formula	$C_{23}H_{27}N_3O_3P_3Br_3$	$C_{23}H_{27}N_3O_3P_3Br_3$
fw	726.1	726.1
space group	$P\bar{1}$	$P2_1/n$
a (Å)	9.872(4)	12.721(6)
b (Å)	13.438(6)	13.468(7)
c (Å)	13.548(8)	17.882(5)
α (deg)	117.02(5)	
β (deg)	96.00(6)	101.62(3)
γ (deg)	105.38(4)	
V (Å^3)	1490(2)	3001(2)
Z	2	4
ρ_c (g·cm^{-3})	1.619	1.607
T (°C)	18	18
μ(Mo Kα) (cm^{-1})	42.1	41.8
λ(Mo Kα) (Å)	0.7107	0.7107
R^a	0.080	0.066
R_w^b	0.083	0.069

^{a} $R = \sum||F_o| - |F_c||/\sum|F_o|$. ^{b} $R_w = [\sum w(|F_o| - |F_c|)^2/\sum w|F_o|^2]^{1/2}$.

Table VII. Atomic Coordinates and Equivalent Isotropic Thermal Parametres for **2a**

atom	x/a	y/b	z/c	10^3U_{eq}[a] (Å^3)
P1	0.4431(5)	0.2682(4)	0.2683(4)	53(3)
N1	0.3880(14)	0.1670(11)	0.1272(11)	52(7)
P2	0.3691(5)	0.1871(4)	0.0124(4)	55(3)
N2	0.5118(14)	0.3108(10)	0.0561(10)	51(7)
P3	0.6021(5)	0.4340(4)	0.1836(4)	53(2)
N3	0.5763(14)	0.3807(11)	0.2732(11)	55(8)
O1	0.3187(12)	0.3340(9)	0.2888(8)	54(6)
C11	0.1915(24)	0.2797(15)	0.2983(14)	68(11)
C12	0.1806(20)	0.2331(15)	0.3769(15)	61(11)
C13	0.0433(26)	0.1799(15)	0.3832(16)	66(13)
C14	−0.0758(20)	0.1686(15)	0.3162(17)	63(11)
C15	−0.0730(20)	0.2126(18)	0.2411(14)	64(12)
C16	0.0578(20)	0.2685(17)	0.2320(15)	61(11)
Br1	0.2633(2)	0.9081(2)	0.6699(2)	91(1)
C1	0.3446(21)	0.0381(14)	0.0970(15)	67(11)
C2	0.1834(18)	−0.0196(17)	0.0724(18)	94(13)
O2	0.2321(11)	0.2365(10)	0.0341(9)	60(7)
C21	0.1659(17)	0.2572(17)	−0.0458(16)	50(12)
C22	0.1683(20)	0.3680(18)	−0.0091(15)	65(12)
C23	0.1004(20)	0.3917(16)	−0.0836(19)	74(12)
C24	0.0239(18)	0.2961(21)	−0.2000(16)	59(11)
C25	0.0275(16)	0.1852(20)	−0.2365(16)	66(13)
C26	0.0969(19)	0.1640(15)	−0.1592(15)	58(10)
Br2	0.0704(3)	0.6704(3)	1.3070(2)	133(2)
C3	0.5539(21)	0.3234(17)	−0.0465(14)	74(11)
C4	0.6642(27)	0.2629(20)	−0.0883(22)	119(19)
O3	0.4814(11)	0.5029(9)	0.1922(8)	50(6)
C31	0.5172(18)	0.6151(15)	0.2840(14)	49(10)
C32	0.6397(17)	0.7112(15)	0.3056(15)	54(11)
C33	0.6669(23)	0.8219(15)	0.3999(17)	71(11)
C34	0.5799(23)	0.8390(17)	0.4728(14)	60(12)
C35	0.5429(20)	0.2571(19)	0.5488(14)	64(12)
C36	0.4308(16)	0.6330(13)	0.3588(14)	43(10)
Br3	−0.6325(2)	0.0078(2)	0.3974(2)	82(1)
C5	0.6700(19)	0.4710(15)	0.3997(14)	73(10)
C6	0.7976(21)	0.4395(20)	0.4223(16)	90(14)

^{a} $U_{eq} = {}^1/_3\sum_i\sum_j U_{ij}a^*_i a^*_j \vec{a}_i\vec{a}_j$.

a least-squares procedure. Three strong, well-separated reflections, measured after every 1 h, revealed a drastic decrease in the intensities for both the isomers as the crystals were found to be unstable to X-rays. The extent of crystal decay for **2a** was 54% and for **2b** was 49%. Two crystals were used to complete the data collection of **2a**. The data were corrected for Lorentz, polarization, and absorption effects.[29] Data

Table VIII. Atomic Coordinates and Equivalent Thermal Parameters for **2b**

atom	x/a	y/b	z/c	10^3U_{eq}[a] (Å^3)
P1	0.6048(5)	0.0018(5)	0.7978(3)	71(3)
P2	0.6085(5)	−0.2231(5)	0.8095(4)	77(3)
P3	0.8158(4)	−0.1077(6)	0.8428(4)	75(3)
N1	0.5766(11)	−0.1135(12)	0.7647(8)	63(7)
N2	0.7374(15)	−0.2005(14)	0.8485(11)	103(10)
N3	0.7323(13)	−0.0159(14)	0.8429(10)	83(9)
O1	0.5544(14)	0.0063(11)	0.8741(7)	78(7)
O2	0.5607(13)	−0.2132(11)	0.8886(7)	87(7)
O3	0.8121(13)	−0.1163(20)	0.7523(10)	177(13)
C11	0.4501(22)	0.0349(16)	0.8716(13)	59(11)
C12	0.4310(17)	0.0775(16)	0.9363(12)	65(10)
C13	0.3255(20)	0.1025(16)	0.9439(12)	70(10)
C14	0.2440(17)	0.0825(16)	0.8795(16)	74(11)
C15	0.2612(22)	0.0438(18)	0.8127(13)	82(12)
C16	0.3677(22)	0.0183(19)	0.8088(13)	94(12)
Br1	0.1012(2)	0.1157(3)	0.8878(2)	125(1)
C21	0.4603(18)	−0.2504(17)	0.8975(15)	64(11)
C22	0.3731(23)	−0.2411(18)	0.8360(12)	87(13)
C23	0.2738(21)	−0.2771(21)	0.8437(16)	97(12)
C24	0.2679(20)	−0.3168(19)	0.9164(19)	85(13)
C25	0.3567(27)	−0.3270(22)	0.9734(13)	102(13)
C26	0.4557(24)	−0.2909(16)	0.9644(12)	80(13)
Br2	0.1317(2)	−0.3680(3)	0.9240(2)	136(2)
C31	0.9034(24)	−0.1246(33)	0.7218(14)	109(17)
C32	0.9292(23)	−0.0312(33)	0.6978(17)	113(19)
C33	1.0157(28)	−0.0208(19)	0.6625(15)	92(15)
C34	1.0767(20)	−0.1028(29)	0.6572(11)	68(11)
C35	1.0545(23)	−0.1952(26)	0.6794(15)	88(15)
C36	0.9695(33)	−0.2047(20)	0.7111(19)	124(17)
Br3	1.2037(2)	−0.1092(3)	0.6159(2)	135(1)
C1	0.5122(19)	−0.1206(18)	0.6820(10)	95(11)
C2	0.5870(23)	−0.1271(22)	0.6275(13)	136(16)
C3	0.8153(22)	−0.3186(28)	0.8657(19)	144(19)
C4	0.7918(30)	−0.3110(36)	0.9309(18)	215(24)
C5	0.7897(20)	0.0899(23)	0.8669(17)	122(15)
C6	0.7989(28)	0.1006(26)	0.9465(19)	176(21)

^{a} $U_{eq} = {}^1/_3\sum_i\sum_j U_{ij}a^*_i a^*_j \vec{a}_i\vec{a}_j$.

collection parameters and details of the crystallographic analysis for the *cis* and *trans* isomers (**2a,b**) are summarized in Table VI. The structures of both the isomers were solved by direct methods using SHLEXS-86.[30] Least-squares refinements were performed by full-matrix method on $|F_o|$s using SHELX-76.[30] The atomic scattering factors for the neutral atoms used were those in SHELX-76. Of 27 hydrogens atoms, only 12 appeared in the successive difference maps for **2a** and none for **2b**. For **2a**, anisotropic refinement on non-hydrogen atoms and isotropic refinement on hydrogen atoms converged at $R = 0.080$ and $R_w = 0.083$ for 1659 reflections with $F > 10\sigma(F)$ and 325 variables. For **2b**, the refinement converged at $R = 0.066$ and $R_w = 0.069$ for 1234 observed reflections with $F > 6.0\sigma(F)$ and 325 variables. The final atomic coordinates of **2a,b** are listed in Tables VII and VIII, respectively.

Acknowledgment. We thank Mr. Animesh Pramanik for his help in computing some of the *ab initio* results.

Supplementary Material Available: Tables of full experimental details of the structure determinations, anisotropic thermal parameters, and complete bond distances, bond angles, and least-squares planes for **2a,b**, MNDO optimized geometries for **7** and **8**, and MNDO energies for **7** and **8** (18 pages). Ordering information is given on any current masthead page.

(29) North, A. C. T.; Philips, D. C.; Mathews, F. S. *Acta Crystallogr.* **1968**, *A24*, 351.
(30) (a) Sheldrick, G. M. SHELXS-86: Program for Crystal Structure Solution. University of Goettingen, Germany, 1986. (b) Sheldrick, G. M. SHELX-76: Program for Crystal Structure determination. University of Cambridge, U.K., 1976.